

Improved description of di-lepton production in $\tau^- \rightarrow \nu_\tau P^-$ decays

Adolfo Guevara^{1, 2}, Gabriel López Castro³ and Pablo Roig³

¹ Departamento de Física Atómica, Molecular y Nuclear
 and Instituto Carlos I de Física Teórica y Computacional
 Universidad de Granada, E-18071 Granada, Spain.

² Departament de Física Teòrica, IFIC,
 Universitat de València - CSIC,

Apt. Correus 22085, E-46071 València, Spain

³ Departamento de Física, Centro de Investigación
 y Estudios Avanzados del Instituto Politécnico Nacional.
 AP 14-740, 07000, Ciudad de México, México

November 22, 2021

Abstract Recently, the Belle collaboration reported the first measurements of the $\tau^- \rightarrow \nu_\tau \pi^- e^+ e^-$ branching fraction and the spectrum of the pion-dielectron system. This decay and the corresponding di-muon channel offer the possibility to extract information on the $W\pi\gamma^*$ vertex in a kinematical region relevant for the evaluations of the radiative corrections to $\tau^- \rightarrow \nu_\tau \pi^-$ and of the pion pole part of the hadronic light-by-light contribution to a_μ . This is the motivation to seek for improvements on our previous evaluation of $\tau^- \rightarrow \nu_\tau \pi^- \ell^+ \ell^-$ decays ($\ell = e, \mu$). In this paper we ameliorate our calculation of the $WP^- \gamma^*$ vertex by including flavor symmetry breaking effects in the framework of the Resonance Chiral Theory. We impose QCD short-distance behavior to constrain most parameters and data on the $\pi^- e^+ e^-$ spectrum reported by Belle to fix the remaining free ones. As a result, improved predictions for the branching ratios and hadronic/leptonic spectra are reported, in good agreement with observations. Analogous calculations for the strangeness-changing $\tau^- \rightarrow \nu_\tau K^- \ell^+ \ell^-$ transitions are reported for the first time.

1 Introduction

The search for signals of physics beyond the Standard Model (SM) requires a good understanding of SM processes either to discard possible backgrounds coming from it, such as large radiative corrections [1, 2, 3] or to have under

good control hadronic contamination in precision tests of the SM [4]. In addition to offering a clean laboratory to test the hadronization of the weak currents, semileptonic τ lepton decays provide a good example where SM effects can be reliably calculated to disentangle possible New Physics signals hidden in precision observables.

In Ref. [5] we reported the first prediction of $\mathcal{B}(\tau \rightarrow \nu_\tau \pi \ell \bar{\ell})$ and the corresponding di-lepton spectrum where $\ell = e, \mu$ (this can be viewed as the crossed channels of lepton pairs produced in $(\pi, K)_{\ell 2}$ decays [6] in a larger kinematical domain); later on the Belle collaboration [7] announced the first searches of these decays. Recently, some of us have also reported similar studies of $\tau^- \rightarrow \nu_\tau \pi^- \pi^0 \ell \bar{\ell}$ decays [8]. Together with the five lepton decays of tau leptons [9], they provide a better description of possible backgrounds in Lepton Number- or Lepton Flavor Violation searches in τ decays. Motivated by the Belle Collaboration studies [7], in this work we revisit our predictions for $\tau \rightarrow \nu_\tau \pi \ell \bar{\ell}$ decays with the aim of improving the theoretical description of structure-dependent effects and to get reduced uncertainties. In addition, we make for the first time an analogous analysis of the strangeness-changing processes $\tau \rightarrow \nu_\tau K \ell \bar{\ell}$ as well.

In these phenomena, the $W\gamma^*P$ vertex plays a central role and its description is necessary to understand the radiative corrections to the $\tau^- \rightarrow \nu_\tau P^-$ decays [10]. This vertex also involves parameters which are needed to describe the pion transition form factor, which is required to compute the dominant piece of the hadronic light-by-light contribution to the anomalous magnetic moment of the μ lepton, a_μ . Knowledge on these parameters could also help us to reduce the uncertainty on the hadronic part of a_μ [11].

The problem with the description of these effective vertices arises when one tries to describe them in terms of the fundamental fields of the Standard Model, since at energies below the m_τ scale, one can not give a proper perturbative description of color interactions. The decay amplitude involving these vertices can, however, be split into a part where the pseudo Goldstone boson is treated as a point-like particle and another one depending on the internal structure of hadronic particles and vertices. Thus, we try to surpass the difficulties of calculating the structure-dependent part using Resonance Chiral Theory (R χ T) [12, 13], which is an extension of Chiral Perturbation Theory (χ PT) [14, 15, 16] that includes resonances as active degrees of freedom. χ PT relies on the chiral symmetry group $G = U(3)_L \otimes U(3)_R$ of the massless QCD Lagrangian. After it gets spontaneously broken, $G \rightarrow U(3)_V$, the remaining symmetry gets explicitly broken when the masses of the light quarks are considered to be non-vanishing. The $\mathcal{B}(\tau^- \rightarrow \nu_\tau \pi^- \ell \bar{\ell})$ and di-lepton spectrum were computed previously in ref. [5] using such techniques, however, the novelty in the present treatment is that we include the effects of finite different light-quark masses as done for the Transition Form Factor of the pseudo Goldstone bosons for the Hadronic Light-by-Light part of the a_μ in ref. [17] (over [18], where these were neglected). We also give a more thorough treatment of the uncertainties than those in ref. [5],

thus obtaining consistent results comparing with the corresponding form factors given in ref. [19]. Furthermore, the recent measurement of the branching fraction with a lower limit in the invariant mass of the pion and di-lepton pair [7], $m_{\pi e^- e^+}$, motivates further this re-analysis, since in the $m_{\pi e^- e^+} \geq 1.05$ GeV region the branching fraction gets saturated by the structure-dependent contribution. While most of the parameters of the model can be constrained by means of the high-energy behavior of QCD, some of them remain loose. We fit these to the measured invariant mass $m_{\pi e^- e^+}$ spectra, using also the measurement of the branching fraction $\mathcal{B}(m_{\pi e^- e^+} \geq 1.05 \text{ GeV}) = (5.90 \pm 1.01) \times 10^{-5}$ [7]. As a result, we improve our predictions, with correspondingly reduced uncertainties.

The outline of the paper is as follows. In section 2 the different contributions to the matrix element are collected. In section 3 we introduce the Lagrangian used for computing the structure-dependent corrections, calculate the corresponding form factors (including flavor-breaking corrections to our previous results) and derive the short-distance constraints among resonance couplings. In section 4 we carry out our phenomenological analysis, including a fit to Belle $\tau^- \rightarrow \pi^- e^+ e^- \nu_\tau$ data and predicting the partner ($\pi \leftrightarrow K, e \leftrightarrow \mu$) modes, yet to be discovered. We give our conclusions in section 5.

2 Amplitudes

There are three kinds of contributions to the decay amplitude: the first called inner bremsstrahlung (IB) or structure independent (SI). The other two are the structure dependent (SD) ones, namely the polar- (V) and axial-vector (A) parts of the left-handed weak charged current. The IB amplitude is obtained by treating the pseudo Goldstone bosons as point-like particles, where the photon is either radiated by the τ lepton, off the pseudo Goldstone boson (π or K) or by the longitudinal propagation mode of the W^- boson, a contribution which is needed to achieve gauge invariance of the total IB amplitude¹. The total IB contribution is shown in eq. (1), along with the parametrization of the SD parts as given in ref. [5]. The momenta definition is given in Figure 1.

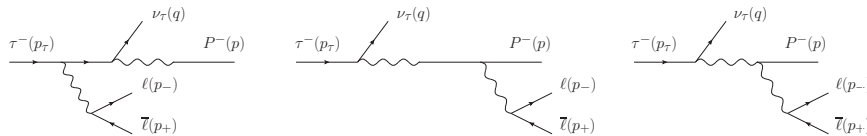


Figure 1: Feynman diagrams of the SI contributions (only scalar QED is used for the radiation off the P^- meson) to the $\tau^-(p_\tau) \rightarrow \nu_\tau(q)P^-(p)\ell(p_-)\bar{\ell}(p_+)$ decay amplitude.

The different contributions to the matrix element are ($D = d, s$ for $P =$

¹The contributions for point-like pseudo Goldstone bosons can be obtained by means of the scalar QED Lagrangian.

π, K)

$$\mathcal{M}_{IB} = -iG_F V_{uD} f m_\tau \frac{e^2}{k^2} J_\ell^\nu \bar{u}_{\nu\tau} (1 + \gamma_5) \left[\frac{2p_\nu}{2p \cdot k + k^2} + \frac{2p_{\tau\nu} - \not{k}\gamma_\nu}{-2p_\tau \cdot k + k^2} \right] u_\tau, \quad (1a)$$

$$\mathcal{M}_V = -G_F V_{uD} \frac{e^2}{k^2} J_\ell^\nu J_\tau^\mu F_V(W^2, k^2) \varepsilon_{\mu\nu\alpha\beta} k^\alpha p^\beta, \quad (1b)$$

$$\mathcal{M}_A = iG_F V_{uD} \frac{e^2}{k^2} J_\ell^\nu J_\tau^\mu \left\{ F_A(W^2, k^2) [(W^2 + k^2 - m_\pi^2) g_{\mu\nu} - 2k_\mu p_\nu] \right. \\ \left. - A_2(W^2, k^2) k^2 g_{\mu\nu} + A_4(W^2, k^2) k^2 (p + k)_\mu p_\nu \right\}. \quad (1c)$$

Here, $J_\ell^\nu = \bar{u}(p_-)\gamma^\nu v(p_+)$ and $J_\tau^\mu = \bar{u}(q)(1 + \gamma_5)\gamma^\mu u(p_\tau)$ are the lepton electromagnetic and τ weak charged currents, respectively. We use $W^2 \equiv (p_\tau - q)^2$ and $k^2 \equiv (p_- + p_+)^2$ as the two independent Lorentz-invariants upon which the form factors (F_V, F_A, A_2, A_4) depend. In ref. [5] the axial amplitude was given only in terms of three form factors (F_V, F_A and a combination of A_2 and A_4 called B), since at chiral order p^4 , the A_2 and A_4 form factors are linearly dependent and can be written in terms of the pseudo Goldstone electromagnetic form factor $F_V^P(k^2)$ [6]. Here, A_2 and A_4 cannot be recast in terms of $F_V^P(k^2)$, since we are considering contributions of chiral order p^6 . Furthermore, including the complete set of leading-order chiral symmetry breaking contributions will change the pion pole for the massive pion propagator. As a result, the A_2 and A_4 form factors become linearly independent and the axial-vector part of the left hadronic current cannot be expressed in terms of the two form factors $\mathcal{F}(W^2, k^2, p^2)$ and $\mathcal{G}(W^2, k^2, p^2)$ of refs. [19, 20, 21] (see discussion after eq. (22)).

3 Structure dependent form factors

3.1 The relevant operators

In this section we will present, for the sake of simplicity, only the relevant operators in the $R\chi T$ Lagrangian needed to compute the form factors, which are given in the next subsection. We will be concise here, for a more extended discussion see eg. ref. [17]. $R\chi T$ extends the domain of applicability of Chiral Perturbation Theory [16, 14, 15] (χPT) by adding the light-flavored resonances as active degrees of freedom.

We start with operators involving no resonances, these being ²

$$\mathcal{L}_{0Res} = \frac{f^2}{4} \langle u^\mu u_\mu + \chi_+ \rangle + \mathcal{L}_{WZW} + C_7^W \mathcal{O}_7^W + C_{11}^W \mathcal{O}_{11}^W + C_{22}^W \mathcal{O}_{22}^W, \quad (2)$$

²Although these terms also appear in the χPT Lagrangian, their couplings get shifted in the presence of resonance contributions (see for instance [22, 23, 24]).

where the first term is given by the leading χ PT Lagrangian operators of chiral order p^2 [16, 14, 15], the second one is the anomalous Wess-Zumino-Witten Lagrangian of $\mathcal{O}(p^4)$ [25, 26] and the last three operators belong to the subleading odd-intrinsic parity sector $\mathcal{O}(p^6)$ Lagrangian [27]. We neglect operators not included in this Lagrangian. Congruently with refs. [19], [21] and [28], we will not consider any $\mathcal{O}(p^8)$ contribution whatsoever. In the first term, f is the decay constant in the chiral limit, which we will set to $f = f_\pi \sim 92$ MeV, u^μ and χ_+ are chiral tensors [29], the former containing derivatives of the π/K fields and external spin-one currents and the latter scalar currents involving the previous fields masses squared, $m_{\pi/K}^2$, times even powers of such fields.

The equations of motion of the resonances give their classical fields in terms of series of chiral tensors of different order. The resonances are said to be integrated out when the classic fields are substituted in favor of these chiral tensors in the resonant Lagrangian. Integrating the resonances out using the leading-order terms of the equations of motion saturates the $\mathcal{O}(p^4)$ (and leading $\mathcal{O}(p^6)$) contributions in the even-intrinsic parity sector [12, 13, 19]; therefore, we will not use the non-resonant $\mathcal{O}(p^4)$ set of operators in order to avoid double counting. Since we will only consider leading-order terms in the resonances equations of motion, the $\mathcal{O}(p^6)$ chiral low-energy constants in the odd-intrinsic parity sector cannot be saturated upon resonance exchange [28], therefore we have to include the three contributing $C_i^W \mathcal{O}_i^W$ terms [27]:

$$\begin{aligned}\mathcal{O}_7^W &= i\epsilon_{\mu\nu\alpha\beta}\langle\chi_- f_+^{\mu\nu} f_+^{\alpha\beta}\rangle, \\ \mathcal{O}_{11}^W &= i\epsilon_{\mu\nu\alpha\beta}\langle\chi_+[f_+^{\mu\nu}, f_-^{\alpha\beta}]\rangle, \\ \mathcal{O}_{22}^W &= i\epsilon_{\mu\nu\alpha\beta}\langle u^\mu\{\nabla_\rho f_+^{\rho\nu}, f_+^{\alpha\beta}\}\rangle,\end{aligned}\tag{3}$$

where the following chiral tensors [29] enter: χ_- gives odd powers of the π/K fields with factors involving m_π^2 or m_K^2 , ∇_μ is the covariant derivative and includes spin-one left and vector external currents through the connection and $f_\pm^{\mu\nu}$ yields the field-strength tensors of the charged-weak or electromagnetic fields.

We turn next to those operators with one resonance field, in either intrinsic parity sector,

$$\mathcal{L}_{1Res} = \mathcal{L}_{1Res}^{even} + \mathcal{L}_{1Res}^{odd}.\tag{4}$$

In turn, the first piece can be further divided according to the quantum numbers of this resonance

$$\mathcal{L}_{1Res}^{even} = \sum_{R_i=V,A,P} \mathcal{L}_{1R_i}^{even}.\tag{5}$$

The contributions with one vector resonance read ³ [12, 19]

$$\mathcal{L}_{1V}^{even} = \frac{F_V}{2\sqrt{2}}\langle V_{\mu\nu} f_+^{\mu\nu}\rangle + \frac{i}{2\sqrt{2}}G_V\langle V_{\mu\nu}[u^\mu, u^\nu]\rangle + \frac{\lambda_V}{\sqrt{2}}\langle V_{\mu\nu}\{f_+^{\mu\nu}, \chi_+\}\rangle,\tag{6}$$

³ $V_{\mu\nu}$ (analogously $A_{\mu\nu}$ for axial resonances below) is a matrix in flavor (u, d, s) space and we use the antisymmetric tensor formalism for spin-one fields for convenience [12, 13].

where the first two operators are of chiral order p^2 , and the last one of $\mathcal{O}(p^4)$. Our $\lambda_V = \sqrt{2}\lambda_6^V$, using the notation in ref. [19]. This last operator is the only one included from the full basis of the $\mathcal{O}(p^4)$ even-intrinsic parity operators in ref. [19] since it is the single one that can contribute to the $U(3)_V$ breaking in the $V - \gamma$ coupling. There are, however, two reasons to disregard the $\mathcal{O}(p^4)$ operators in the even-intrinsic parity sector: The operators that are relevant to the process can be dismissed on the basis of resonance field redefinitions⁴; if we, however, keep such operators, they will only give subleading contributions to those from the first two operators in eq. (6) with no contribution to $U(3)_V$ -breaking vertices.

The axial resonance operators present a similar feature. This is, the $\mathcal{O}(p^4)$ one-resonance even-intrinsic parity operators can be absorbed through field redefinitions [19]. We will therefore disregard any contribution from this part of the Lagrangian, including the $U(3)_V$ breaking terms to the axial-vector resonance coupling to external currents, namely, the JA vertex. The remaining contributions with one resonance field are [12]

$$\mathcal{L}_{1A/P}^{even} = \frac{F_A}{2\sqrt{2}} \langle A_{\mu\nu} f_-^{\mu\nu} \rangle + id_m \langle P\chi_- \rangle, \quad (7)$$

with P a matrix in three-flavors space containing the lightest pseudoscalar resonances. The inclusion of the pseudoscalar resonance is necessary in order to obtain consistent short-distance constraints in $\langle VAP \rangle$ and $\langle VJP \rangle$ Green's functions [19, 28, 30, 31]. All Feynman diagrams involving these resonances will give $U(3)$ breaking contributions to the amplitude due to the last term in eq. (7). We have neglected other spin-zero resonance contributions (scalar and heavier pseudoscalar resonances [5]), which are not needed for theoretical consistency and are irrelevant phenomenologically. The odd-intrinsic parity contributions to \mathcal{L}_{1Res} are [32]⁵

$$\mathcal{L}_{1Res}^{odd} = \sum_{j=1}^7 \frac{c_j}{M_V} \mathcal{O}_V^j + \varepsilon_{\mu\nu\alpha\beta} \langle \kappa_5^P \{ f_+^{\mu\nu}, f_+^{\alpha\beta} \} P \rangle, \quad (8)$$

⁴The λ_V operator also gets absorbed in the field redefinition, however, we keep it in order to show the full basis of possible $U(3)_V$ breaking operators since we do not consider the full even-intrinsic parity $\mathcal{O}(p^6)$ basis. We will show later that this is consistent, since the short distance constraints give $\lambda_V = 0$.

⁵Since we are only considering operators with one π/K field, these constitute a basis. In the general case, the basis is given in ref. [28]. The translation between them can be read from ref. [30].

with the operators

$$\begin{aligned}
\mathcal{O}_V^1 &= \varepsilon_{\mu\nu\rho\sigma} \langle \{V^{\mu\nu}, f_+^{\rho\alpha}\} \nabla_\alpha u^\sigma \rangle, \\
\mathcal{O}_V^2 &= \varepsilon_{\mu\nu\rho\sigma} \langle \{V^{\mu\alpha}, f_+^{\rho\sigma}\} \nabla_\alpha u^\nu \rangle, \\
\mathcal{O}_V^3 &= i\varepsilon_{\mu\nu\rho\sigma} \langle \{V^{\mu\nu}, f_+^{\rho\sigma}\} \chi_- \rangle, \\
\mathcal{O}_V^4 &= i\varepsilon_{\mu\nu\rho\sigma} \langle V^{\mu\nu} [f_-^{\rho\sigma}, \chi_+] \rangle, \\
\mathcal{O}_V^5 &= \varepsilon_{\mu\nu\rho\sigma} \langle \{\nabla_\alpha V^{\mu\nu}, f_+^{\rho\alpha}\} u^\sigma \rangle, \\
\mathcal{O}_V^6 &= \varepsilon_{\mu\nu\rho\sigma} \langle \{\nabla_\alpha V^{\mu\alpha}, f_+^{\rho\sigma}\} u^\nu \rangle, \\
\mathcal{O}_V^7 &= \varepsilon_{\mu\nu\rho\sigma} \langle \{\nabla^\sigma V^{\mu\nu}, f_+^{\rho\alpha}\} u_\alpha \rangle.
\end{aligned} \tag{9}$$

In the following, we quote those terms bilinear in resonance fields (we do not display the kinetic terms for the resonances, which can be found in ref. [12], as they do not contribute to the effective vertices).

$$\mathcal{L}_{2\text{Res}} = \mathcal{L}_{2\text{Res}}^{\text{even}} + \mathcal{L}_{2\text{Res}}^{\text{odd}}, \tag{10}$$

with [19, 33, 34, 35]⁶

$$\mathcal{L}_{2\text{Res}}^{\text{even}} = -e_M^V \langle V_{\mu\nu} V^{\mu\nu} \chi_+ \rangle + \lambda_1^{PV} \mathcal{O}_1^{PV} + \lambda_2^{PV} \mathcal{O}_2^{PV} + \lambda_1^{PA} \mathcal{O}_1^{PA} + \sum_{i=1}^5 \lambda_i^{VA} \mathcal{O}_i^{VA}, \tag{11}$$

and [28, 32]

$$\mathcal{L}_{2\text{Res}}^{\text{odd}} = \sum_{i=1}^3 d_i \mathcal{O}_i^{VV} + \kappa_3^{PV} \mathcal{O}_3^{PV}. \tag{12}$$

The operators appearing in the two previous equations are ($h^{\mu\nu} = \nabla^\mu u^\nu + \nabla^\nu u^\mu$)

$$\begin{aligned}
\mathcal{O}_1^{PV} &= i \langle [\nabla^\mu P, V_{\mu\nu}] u^\nu \rangle, \\
\mathcal{O}_2^{PV} &= i \langle [P, V_{\mu\nu}] f_-^{\mu\nu} \rangle; \\
\mathcal{O}_1^{PA} &= i \langle [P, A_{\mu\nu}] f_+^{\mu\nu} \rangle; \\
\mathcal{O}_1^{VA} &= \langle [V^{\mu\nu}, A_{\mu\nu}] \chi_- \rangle, \\
\mathcal{O}_2^{VA} &= i \langle [V^{\mu\nu}, A_{\nu\alpha}] h_\mu^\alpha \rangle, \\
\mathcal{O}_3^{VA} &= i \langle [\nabla^\mu V_{\mu\nu}, A^{\nu\alpha}] u_\alpha \rangle, \\
\mathcal{O}_4^{VA} &= i \langle \nabla^\alpha V_{\mu\nu}, A_\alpha^\nu \rangle u^\mu, \\
\mathcal{O}_5^{VA} &= i \langle [\nabla^\alpha V_{\mu\nu}, A^{\mu\nu}] u_\alpha \rangle; \\
\mathcal{O}_1^{VV} &= \varepsilon_{\mu\nu\rho\sigma} \langle \{V^{\mu\nu}, V^{\rho\alpha}\} \nabla_\alpha u^\sigma \rangle, \\
\mathcal{O}_2^{VV} &= i\varepsilon_{\mu\nu\rho\sigma} \langle \{V^{\mu\nu}, V^{\rho\sigma}\} \chi_- \rangle, \\
\mathcal{O}_3^{VV} &= \varepsilon_{\mu\nu\rho\sigma} \langle \{\nabla_\alpha V^{\mu\nu}, V^{\rho\alpha}\} u^\sigma \rangle, \\
\mathcal{O}_3^{PV} &= \varepsilon_{\mu\nu\alpha\beta} \langle \{V^{\mu\nu}, f_+^{\alpha\beta}\} P \rangle.
\end{aligned} \tag{13}$$

⁶The operator with coefficient e_M^V allows to account for $U(3)$ breaking effects in the vector resonance masses, in agreement with phenomenology.

There is only one relevant operator with three resonance fields in either parity sector

$$\mathcal{L}_{3Res} = i\lambda^{VAP} \langle [V_{\mu\nu}, A^{\mu\nu}] P \rangle + \kappa^{PVV} \varepsilon_{\mu\nu\rho\sigma} \langle V^{\mu\nu} V^{\alpha\beta} P \rangle. \quad (14)$$

3.2 Form Factors

In this section we quote our results for the different contributions to the F_V , F_A , A_2 , A_4 form factors, for $P = \pi, K$. All resonance propagators are to be understood as provided with an energy-dependent width ($M_R^2 - x \rightarrow M_R^2 - x - iM_R\Gamma_R(x)$, $x = W^2, k^2$) computed within $R\chi T$, using those in refs. [36] ($\rho(770)$), [37] ($K^*(892)$) and [38, 39] ($a_1(1260)$), including the $KK\pi$ cuts [40]. A constant width will suffice for the very narrow $\omega(782)$ and $\phi(1020)$ mesons (their PDG [41] values will be taken). For the $K_1(1270/1400)$ states we will follow [42].

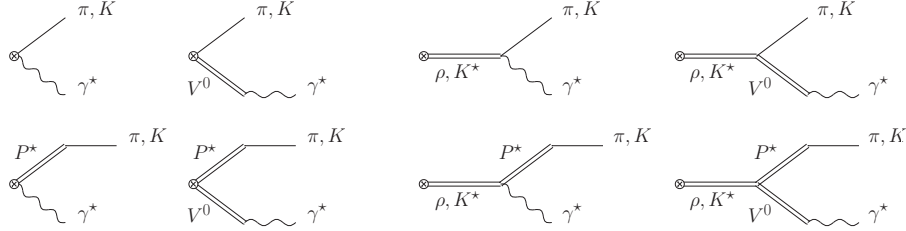


Figure 2: Feynman diagrams contributing to the vector part of the left hadronic current. The resonance P^* is the pseudoscalar resonance corresponding to $\pi(1300) \equiv \pi'$ ($K(1460) \equiv K'$) for $P = \pi(K)$. The resonance V^0 means ω for $P = \pi$ and ρ^0, ω, Φ for $P = K$.

The vector form factors are ($N_C = 3$ in QCD)

$$F_V^{(\pi)}(W^2, k^2) = \frac{1}{3f} \left\{ -\frac{N_C}{8\pi^2} + 64m_\pi^2 C_7^{W^*} - 8C_{22}^W(W^2 + k^2) \right. \\ + \frac{4F_V^{ud^2}}{M_\rho^2 - W^2} \frac{d_3(W^2 + k^2) + d_{123}^* m_\pi^2}{M_\omega^2 - k^2} \\ + \frac{2\sqrt{2}F_V^{ud}}{M_V} \frac{c_{1256} W^2 - c_{1235}^* m_\pi^2 - c_{125} k^2}{M_\rho^2 - W^2} \\ \left. + \frac{2\sqrt{2}F_V^{ud}}{M_V} \frac{c_{1256} k^2 - c_{1235}^* m_\pi^2 - c_{125} W^2}{M_\omega^2 - k^2} \right\}, \quad (15)$$

$$F_V^{(K)}(W^2, k^2) = \frac{1}{f} \left\{ -\frac{N_C}{24\pi^2} + \frac{64}{3} m_K^2 C_7^{W^*} + 32C_{11}^W \Delta_{K\pi}^2 - \frac{8}{3} C_{22}^W(W^2 + k^2) \right\}$$

$$\begin{aligned}
& + \frac{2F_V^{us} [d_3(W^2 + k^2) + d_{123}^* m_K^2]}{M_{K^*}^2 - W^2} \left(\frac{F_V^{ud}}{M_\rho^2 - k^2} + \frac{1}{3} \frac{F_V^{ud}}{M_\omega^2 - k^2} - \frac{2}{3} \frac{F_V^{ss}}{M_\phi^2 - k^2} \right) \\
& + \frac{2\sqrt{2}F_V^{us} c_{1256}W^2 - c_{1235}^* m_K^2 - c_{125}k^2 + 24c_4\Delta_{K\pi}^2}{3M_V} \frac{1}{M_{K^*}^2 - W^2} \\
& + \frac{\sqrt{2} (c_{1256}k^2 - c_{1235}^* m_K^2 - c_{125}W^2)}{M_V} \left(\frac{F_V^{ud}}{M_\rho^2 - k^2} + \frac{1}{3} \frac{F_V^{ud}}{M_\omega^2 - k^2} - \frac{2}{3} \frac{F_V^{ss}}{M_\phi^2 - k^2} \right) \Bigg\}, \tag{16}
\end{aligned}$$

where $\Delta_{K\pi}^2 = m_K^2 - m_\pi^2$ and we have used the combinations of coupling constants [43]

$$c_{125} = c_1 - c_2 + c_5,$$

$$c_{1256} = c_1 - c_2 - c_5 + 2c_6,$$

$$c_{1235} = c_1 + c_2 + 8c_3 - c_5,$$

$$d_{123} = d_1 + 8d_2 - d_3.$$

$F_V^{uD,ss}$ and starred coefficients absorb $U(3)$ breaking contributions induced by λ_V in eq. (6) and pseudoscalar resonances, respectively. Their expressions are given at the end of this subsection, after eq. (22).

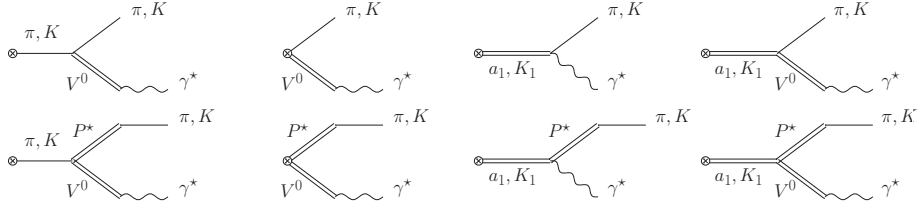


Figure 3: Feynman diagrams contributing to the axial part of the left hadronic current. Conventions for P^* is the same as in the previous figure, the resonance V^0 means ρ^0 for $P = \pi$ and ρ^0, ω, Φ for $P = K$.

The axial form factors are ⁷

$$\begin{aligned}
F_A^{(\pi)}(W^2, k^2) &= \frac{F_V^{ud} F_V^{ud} - 2G_V - m_\pi^2 \frac{4\sqrt{2}d_m}{M_\pi^2} (\lambda_1^{PV} + 2\lambda_2^{PV})}{2f} \frac{1}{M_\rho^2 - k^2} \\
&- \frac{F_A F_A - 2m_\pi^2 \frac{4\sqrt{2}d_m}{M_\pi^2} \lambda_1^{PA}}{2f} \frac{1}{M_{a_1}^2 - W^2} + \frac{\sqrt{2}}{f} \frac{F_A F_V^{ud}}{M_{a_1}^2 - W^2} \frac{\lambda_0^* m_\pi^2 - \lambda' k^2 - \lambda'' W^2}{M_\rho^2 - k^2}, \tag{17} \\
F_A^{(K)}(W^2, k^2) &= -\frac{F_A F_A - 2m_K^2 \frac{4\sqrt{2}d_m}{M_{K'}^2} \lambda_1^{PA}}{2f} \frac{1}{M_{K_1}^2 - W^2}
\end{aligned}$$

⁷We note a factor of two typo in writing $F_A^{(\pi)}$ in ref. [5]. The result written here agrees with the one in ref. [44] for $k^2 \rightarrow 0$.

$$\begin{aligned}
& + \left[\frac{\sqrt{2}F_A \lambda_0^* m_K^2 - \lambda' k^2 - \lambda'' W^2}{2f} \frac{F_V^{us} \left(F_V^{us} - 2G_V + m_K^2 \frac{4\sqrt{2}d_m}{M_{K'}^2} (\lambda_1^{PV} + 2\lambda_2^{PV}) \right)}{M_{K_1}^2 - W^2} + \frac{F_V^{us}}{4f} \right] \\
& \times \left(\frac{F_V^{ud}}{M_\rho^2 - k^2} + \frac{1}{3} \frac{F_V^{ud}}{M_\omega^2 - k^2} + \frac{2}{3} \frac{F_V^{ss}}{M_\phi^2 - k^2} \right), \quad (18)
\end{aligned}$$

$$\begin{aligned}
A_2^{(\pi)}(W^2, k^2) = & \\
& \frac{2}{f} \left(G_V + \frac{2\sqrt{2}m_\pi^2 d_m}{M_{\pi'}^2} \lambda_1^{PV} + \frac{\sqrt{2}F_A}{M_{a_1}^2 - W^2} W^2 (\lambda' + \lambda'') \right) \frac{F_V^{ud}}{M_\rho^2 - k^2}, \quad (19)
\end{aligned}$$

$$\begin{aligned}
A_2^{(K)}(W^2, k^2) = & \left(\frac{G_V}{f} + \frac{2\sqrt{2}m_K^2 d_m}{M_{K'}^2} \frac{\lambda_1^{PV}}{f} + \frac{\sqrt{2}F_A}{M_{K_1}^2 - W^2} \frac{W^2 (\lambda' + \lambda'')}{f} \right) \\
& \times \left(\frac{F_V^{ud}}{M_\rho^2 - k^2} + \frac{1}{3} \frac{F_V^{ud}}{M_\omega^2 - k^2} + \frac{2}{3} \frac{F_V^{ss}}{M_\phi^2 - k^2} \right), \quad (20)
\end{aligned}$$

$$\begin{aligned}
A_4^{(\pi)}(W^2, k^2) = & \frac{2}{f} \frac{F_V^{ud}}{M_\rho^2 - k^2} \left[\frac{G_V}{W^2 - m_\pi^2} + \frac{2\sqrt{2}d_m m_\pi^2 \lambda_1^{PV}}{M_\pi^2 (W^2 - m_\pi^2)} + \frac{\sqrt{2}F_A (\lambda' + \lambda'')}{M_{a_1}^2 - W^2} \right], \quad (21)
\end{aligned}$$

$$\begin{aligned}
A_4^{(K)}(W^2, k^2) = & \frac{1}{f} \left(\frac{G_V}{W^2 - m_K^2} + \frac{2\sqrt{2}d_m m_K^2 \lambda_1^{PV}}{M_K^2 (W^2 - m_\pi^2)} + \frac{\sqrt{2}F_A (\lambda' + \lambda'')}{M_{K_1}^2 - W^2} \right) \\
& \times \left(\frac{F_V^{ud}}{M_\rho^2 - k^2} + \frac{1}{3} \frac{F_V^{ud}}{M_\omega^2 - k^2} + \frac{2}{3} \frac{F_V^{ss}}{M_\phi^2 - k^2} \right), \quad (22)
\end{aligned}$$

It is worth to notice that by replacing the P propagator in $A_2^{(P)}$ and $A_4^{(P)}$ with the massless pole propagator, one recovers the linear dependence between both form factors, thus getting a congruent expression with those in reference [19]. Therefore, the short-distance constraints obtained in this reference can be used as shown there if the Weinberg's sum rules are imposed. We, however, do not make use of these sum rules, as $F_{V/A}$ are fitted to data (see discussion in sections 3.3 and 4.2).

We introduced the short-hand notation

$$\begin{aligned}
F_V^{ud} & \equiv F_V + 8m_\pi^2 \lambda_V, \\
F_V^{us} & \equiv F_V + 8m_K^2 \lambda_V,
\end{aligned}$$

$$F_V^{ss} \equiv F_V + 8(2m_K^2 - m_\pi^2)\lambda_V,$$

for the shifts appearing also in [17].⁸

We also used [33]

$$-\sqrt{2}\lambda_0^* = 4\lambda_1^* + \lambda_2 + \frac{\lambda_4}{2} + \lambda_5,$$

$$\sqrt{2}\lambda' = \lambda_2 - \lambda_3 + \frac{\lambda_4}{2} + \lambda_5$$

and

$$\sqrt{2}\lambda'' = \lambda_2 - \frac{\lambda_4}{2} - \lambda_5.$$

We employed several starred coefficients including $U(3)$ breaking contributions, as given below:

$$\lambda_1^* = \lambda_1 - \frac{\lambda^{VAP} d_m}{M_P^2},$$

$$C_7^{W^*} = C_7^W + \frac{\kappa_5^P d_m}{M_P^2},$$

$$c_3^* = c_3 + \frac{\kappa_3^{PV} d_m M_V}{M_P^2},$$

implying

$$c_{1235}^* = c_1 + c_2 + 8c_3^* - c_5, \text{ and}$$

$$d_2^* = d_2 + \frac{\kappa^{VVP} d_m}{2M_P^2},$$

yielding

$$d_{123}^* = d_1 + 8d_2^* - d_3.$$

We have first shown here the correction to λ_1 appearing in λ_1^* , while the remaining starred couplings were already introduced in ref. [17].

We will follow the scheme explained in ref. [42] to account for the mixing between the $K_1(1270) = K_{1L}$ and the $K_1(1400) = K_{1H}$ states. This amounts to replacing, in eq. (18), $(M_{K_1}^2 - W^2)^{-1} \rightarrow \cos^2\theta_A(M_{K_{1H}}^2 - W^2)^{-1} + \sin^2\theta_A(M_{K_{1L}}^2 - W^2)^{-1}$, with mixing angle $\theta_A \in [37, 58]^\circ$.

3.3 Short-distance constraints

We will demand that the different form factors have an asymptotic behaviour in agreement with QCD [45, 46]. Specifically, we will require their vanishing for large λ in the $\lim_{\lambda \rightarrow \infty} F_V(\lambda W^2, 0)$ and $\lim_{\lambda \rightarrow \infty} F_V(\lambda W^2, \lambda k^2)$ cases. We will do this first in the chiral limit and then at $\mathcal{O}(m_P^2)$ ⁹, paralleling the discussion

⁸As mentioned in section 3.1, a similar shift can be introduced in F_A , however, the operator responsible for such shift can be absorbed through axial resonance field redefinitions [19].

⁹Since we are considering a complete basis of chiral symmetry breaking operators at order m_P^2 , we neglect higher-order chiral corrections.

in ref. [17] for the neutral pseudoscalar transition form factors. In this way, we find the following relations:

- $F_V^{(\pi)}(W^2, k^2), \mathcal{O}(m_P^0)$:

$$C_{22}^W = 0, \quad (23)$$

$$c_{125} = 0, \quad (24)$$

$$c_{1256} = -\frac{N_C M_V}{32\sqrt{2}\pi^2 F_V}, \quad (25)$$

$$d_3 = -\frac{N_C M_V^2}{64\pi^2 F_V^2}. \quad (26)$$

- $F_V^{(\pi)}(W^2, k^2), \mathcal{O}(m_P^2)$:

$$\lambda_V = -\frac{64\pi^2 F_V}{N_C} C_7^{W*}, \quad (27)$$

$$c_{1235}^* = \frac{N_C M_V e_m^V}{8\sqrt{2}\pi^2 F_V} + \frac{N_C M_V^3 \lambda_V}{4\sqrt{2}\pi^2 F_V^2}. \quad (28)$$

- $F_V^{(K)}(W^2, k^2), \mathcal{O}(m_P^0)$: Same constraints as for the π case, since both form factors¹⁰ are identical in the $U(3)$ symmetry limit.

- $F_V^{(K)}(W^2, k^2), \mathcal{O}(m_P^2)$:

$$C_{11}^W = \frac{N_C \lambda_V}{64\pi^2 F_V}. \quad (29)$$

For the sake of predictability and in order to further constrain the parameters in the form factor, we use the VVP Green function, $\Pi_{VVP}(r^2, p^2, q^2)$, constraints [28] obtained from the high-energy behaviour when $r^2 \rightarrow \infty, p^2 \rightarrow \infty$ and $q^2 \rightarrow \infty$ and matching to the Operator Product Expansion (OPE) leading terms in the chiral and large- N_C limits. These give

$$c_{125} = c_{1235} = 0, \quad c_{1256} = -\frac{N_C M_V}{32\sqrt{2}\pi^2 F_V},$$

$$\kappa_5^P = 0, \quad d_3 = -\frac{N_C M_V^2}{64\pi^2 F_V^2} + \frac{F^2}{8F_V^2} + \frac{4\sqrt{2}d_m \kappa_3^{PV}}{F_V},$$

$$C_7^W = C_{22}^W = 0, \quad d_{123} = \frac{F^2}{8F_V^2}.$$

¹⁰ F_A^P and $A_{2,4}^P$ form factors are also identical in this limit for $P = \pi$ or K , obviously.

Notice that these constrictions coincide with our expressions in eqs. (23-26) and that they imply

$$\begin{aligned}
C_{11}^W &= \lambda_V = C_7^{W*} = 0, \\
d_{123} &= \frac{F^2}{8F_V^2}, \\
d_m \kappa_3^{PV} &= \frac{N_C e_m^V}{64\sqrt{2}\pi^2 F_V M_\pi^2}.
\end{aligned} \tag{30}$$

On the other hand, no relation among parameters of the axial form factors can be obtained by taking the infinite virtualities limit, since it already has the right asymptotic behavior. Instead, we will rely on the relations obtained using the VAP Green Function¹¹ $\Pi_{VAP}(p^2, q^2, (p+q)^2)$ [21] in an analogous manner to that done for the $\Pi_{VVP}(r^2, p^2, q^2)$ Green Function.

We recall that the simultaneous analysis of the scalar form factor [49, 50] and the SS-PP sum rules [51] yields $d_m = F/(2\sqrt{2})$. Additionally, notice that $A_{2,4}^{(P)}$ depend on λ_1^{PV} . In turn, $F_A^{(P)}$ depends on λ_1^{PA} and $\lambda_1^{PV} + 2\lambda_2^{PV}$. The appropriate short-distance behaviour of the VAP Green Function [21] fixes all of them but λ_0^* or, in other words λ^{VAP} , as noted in ref. [19]

$$\begin{aligned}
\lambda_0 &= \frac{F^2}{4\sqrt{2}F_V F_A}, & \lambda' &= \frac{F^2 + F_A^2}{2\sqrt{2}F_V F_A}, \\
\lambda'' &= -\frac{F^2 + F_A^2 - 2F_V G_V}{2\sqrt{2}F_V F_A}, & d_m \lambda_1^{PV} &= -\frac{F^2}{4\sqrt{2}F_V}, \\
d_m \lambda_2^{PV} &= \frac{3F^2 + 2F_A^2 - 2F_V^2}{16\sqrt{2}F_V}, & d_m \lambda_1^{PA} &= \frac{F^2}{16\sqrt{2}F_A}.
\end{aligned} \tag{31}$$

Despite the relation for d_m from the scalar form factor and the SS-PP Green's function, notice that there is no need for one since d_m always appears multiplied by one of the other parameters to be constrained. We will also make use of the constraint [12]

$$F_V G_V = F^2. \tag{32}$$

In order to gain predictability, we will use the values of d_{123}^* , M_V and e_m^V given for the best fit of reference [17], namely (their correlations are given in the quoted reference)

$$\begin{aligned}
d_{123}^* &= -(2.3 \pm 1.5) \times 10^{-1}, \\
M_V &= (791 \pm 6) \text{ MeV}, \\
e_m^V &= -(0.36 \pm 0.10).
\end{aligned} \tag{33}$$

¹¹See, however, the discussion in section 6.2 of [47] comparing these short-distance constraints to the results in refs. [48, 20].

4 Phenomenological analysis

4.1 Phase space

In order to make a more direct comparison of our results with the Belle data, we will make use of two sets of variables for the phase space: We will use the same as in ref. [5] for comparing with our previous results and another set in which we only change one of the angles for the invariant mass of the W boson, or, in other words, the invariant mass of the pseudo Goldstone boson and the charged lepton pair, $m_{P\ell\bar{\ell}}$. We recall that the variables in ref. [5] are the invariant mass squared of the pseudo Goldstone and the neutrino, $s_{12} = m_{P\nu\tau}^2$, the invariant mass squared of the charged lepton pair, $s_{34} = m_{\ell\bar{\ell}}^2$, and three angles, θ_1 , θ_3 and ϕ_3 , such that

$$\begin{aligned} (m_3 + m_4)^2 &\leq s_{34} \leq (M - m_1 - m_2)^2, \\ (m_1 + m_2)^2 &\leq s_{12} \leq (M - \sqrt{s_{34}})^2, \\ 0 &\leq \theta_{1,3} \leq \pi, \quad 0 \leq \phi_3 \leq 2\pi. \end{aligned}$$

If we identify the particle with tag 1 with ν_τ , the invariant mass of the weak gauge boson relates to s_{34} via

$$W^2 = M_{234}^2 = M^2 + m_1^2 - \frac{(M^2 + s_{12} - s_{34})(s_{12} + m_1^2 - m_2^2)}{2s_{12}} - X\beta_{12} \cos \theta_1, \quad (34)$$

where $\beta_{ij} = \lambda^{1/2}(s_{ij}, m_i^2, m_j^2)/s_{ij}$ and $X = \lambda^{1/2}(M^2, s_{12}, s_{34})/2$, being $\lambda(a, b, c) = a^2 + b^2 + c^2 - 2ab - 2ac - 2bc$, the Källén lambda function. The kinematic limits on the non-angular variables are now

$$m_2 + m_3 + m_4 \leq M_{234} \leq M, \quad (35a)$$

$$(m_3 + m_4)^2 \leq s_{34} \leq (M_{234} - m_2)^2, \quad (35b)$$

$$s_{12}^- \leq s_{12} \leq s_{12}^+, \quad (35c)$$

where

$$\begin{aligned} s_{12}^\pm &= M^2 + m_1^2 + m_2^2 + s_{34} - W^2 + \frac{(M^2 - m_1^2)(m_2^2 - s_{34})}{W^2} \\ &\pm \frac{1}{2W^2} \lambda^{1/2}(M^2, W^2, m_1^2) \lambda^{1/2}(W^2, s_{34}, m_2^2). \end{aligned} \quad (36)$$

With this, the differential decay rate is given as

$$\begin{aligned} d\Gamma(\tau^- \rightarrow \nu_\tau P^- \ell\bar{\ell}) &= \frac{X\beta_{12}\beta_{34}}{4(4\pi)^6 m_\tau^3} \overline{|\mathcal{M}|^2} ds_{34} ds_{12} d(\cos \theta_1) d(\cos \theta_3) d\phi_3 \\ &= \frac{\beta_{34}}{4(4\pi)^6 m_\tau^3} \overline{|\mathcal{M}|^2} dM_{P\ell\bar{\ell}}^2 ds_{34} ds_{12} d(\cos \theta_3) d\phi_3. \end{aligned} \quad (37)$$

4.2 Fit to data

Short-distance QCD behaviour [17, 19] does not constrain all parameters. Thus, we fit some of the remaining unknowns using the invariant mass spectra of the W boson, $m_{\pi^-e^+e^-}$, measured by the Belle collaboration [7]. We start with a four parameters fit (F_V , F_A , λ_0 and \mathcal{B} , the branching fraction, are floated). Despite the fact that the whole $m_{\pi^-e^+e^-}$ spectrum has been measured, not all the data is available for this minimization since points below $m_{\pi^-e^+e^-} < 1.05$ GeV were used as a control region to validate the Monte Carlo simulation, leaving thus the most sensitive part to SD contributions as the signal region [7]; therefore we use for the minimization the data above the cut $m_{\pi^-e^+e^-} = 1.05$ GeV.

We use only the data set for the $\tau^- \rightarrow \pi^-e^+e^-\nu_\tau$ mode¹². Comparison of this with the expected signal events distribution in this reference allows us to roughly quantify the deconvolution of signal from detector, which we ignore. We have assumed this to be an energy-independent effect for simplicity, and taken it into account as a systematic uncertainty in the data. This error turns out to be comparable to the one reported by Belle for the branching fraction measured above the cut. In addition to this, the Belle collaboration used the expressions of our ref. [5]; which however had factors 2 typos in some of the F_A terms. Besides, trying to keep our previous analysis as simple as possible, it resulted incomplete in the sense of *VAP* Green's function analysis¹³, which altogether could lead to biased estimations of the decay observables. Both reasons motivate our choice of fitting the total branching fraction, \mathcal{B} , as an additional parameter instead of simply computing it from the decay width expression in eq. (37).

We used the relation

$$\int dm_{\pi^-e^+e^-} \frac{1}{\Gamma} \frac{d\Gamma}{dm_{\pi^-e^+e^-}} = 1 = \int dm_{\pi^-e^+e^-} \frac{1}{N} \frac{dN}{dm_{\pi^-e^+e^-}} = \sum_{\text{bins}} \frac{1}{N} \frac{N_{\text{bin}}}{\Delta m_{\pi^-e^+e^-}}, \quad (38)$$

where N is the total number of events, N_{bin} is the number of events in a given bin and $\Delta m_{\pi^-e^+e^-}$ is the bin width. We thus minimize the χ^2 given by

$$\chi^2 = \left(\frac{N}{\Gamma} \frac{\Delta m_{\pi^-e^+e^-}}{\varepsilon_{\text{bin}}} \frac{d\Gamma}{dm_{\pi^-e^+e^-}} - \frac{N_{\text{bin}}}{\varepsilon_{\text{bin}}} \right)^2 + \left(\frac{\mathcal{B} - BR}{\varepsilon_{BR}} \right)^2, \quad (39)$$

where ε_{bin} is the experimental uncertainty in a given bin, BR is the branching ratio for $m_{\pi^-e^+e^-} \geq 1.05$ GeV reported by Belle [7], ε_{BR} its error and \mathcal{B} the one obtained integrating our differential decay width above this cut. We recall that $BR(\tau^- \rightarrow \nu_\tau \pi^- e^+ e^-) = (5.90 \pm 0.53 \pm 0.85 \pm 0.11) \times 10^{-6}$ [7], where the

¹²This is the one shown in the plots of ref. [7]. We have checked better agreement with the Monte Carlo simulation (based on our previous paper [5], see also [52, 53]) for this mode with respect to its charge-conjugated mode.

¹³Pseudoscalar resonance exchange and $\mathcal{O}(p^6)$ operators in the $A_2^{(\pi)}$ and $A_4^{(\pi)}$ form factors are lacking in our ref. [5]. This leads to relating both form factors to the π electromagnetic form factor [6].

first uncertainty is statistical, the second is systematic, and the third is due to the model dependence. In our fits, we have first realized that, varying all four parameters, there happen to be many quasidegenerate best fits and that the correlations among the fit parameters (F_V , F_A , λ_0 and \mathcal{B}) are always large. We interpret this as the data not being precise enough to disentangle the physical solutions among all close to the global minimum. Then, we proceeded to further simplify the fits by making constant one of these four parameters (not \mathcal{B} , as our systematic error due to unfolding is comparable to the overall uncertainty of BR).

We present two sets of fits as our reference results. One fixing $F_A = 130$ MeV ($\sim \sqrt{2}F$, in agreement with [30]), and the other setting $\lambda_0^* = 102 \times 10^{-3}$ (which is in the ballpark of previous estimates for λ_0 , and neglects the contribution of pseudoscalar resonances to the starred coupling, see [54] and refs. therein). Considering individually the π^+ or π^- sets we find that, apart from the incompatibility among both sets in several bins, the π^+ data set leads to the unphysical condition $F_A > F_V$. Also, fixing F_V to its short-distance prediction $F_V \sim \sqrt{3}F \sim 159$ MeV [30], yields fits with larger χ^2 that we disregard. One way of interpreting this feature would be that excited resonances (at least the $\rho(1450)$ state and its interference with the $\rho(1700)$ resonance) are needed for an improved description of the data. However, given the errors of the measurement and the lack of $m_{e^+e^-}$ invariant mass distribution data we are not able to test such more sophisticated theory input, which introduces several additional parameters that remain unconstrained after applying the short-distance conditions (see, e. g. ref. [55]). We thus understand that our fitted values of F_V are effectively capturing missing dynamics in our description (such as the $\rho(770)$ excitations).

Our results are shown in table 1, the corresponding $\chi^2/dof \sim 1.2$ is reasonably good and \mathcal{B} is in agreement with the Belle data within less than 1 standard deviation in both cases. According to these results, we cannot exclude that pseudoscalar resonances give sizeable contributions to λ_0^* . We consider both fit results in table 1 as benchmarks for our predictions in the remainder of this work (we will refer to them as 'the two sets'). The difference among the corresponding two results can be taken as a first, rough estimate of our model-dependent error.

4.3 Predictions for the $\tau^- \rightarrow \nu_\tau P^- \ell \bar{\ell}$ decays

By generating 2400 points in the parameter space making a Gaussian variation of parameters, taking into account the correlations among them, we computed the sum of the SD and the SD-SI interference contributions to the branching fractions for the full phase space. We also computed for the $P = \pi$ and $\ell = e$ channel the SI contribution to \mathcal{B} with the cut $m_{\pi^- e^+ e^-} \geq 1.05$ GeV,

$$\mathcal{B}(IB) \Big|_{m_{\pi^- e^+ e^-} \geq 1.05 \text{ GeV}} = (1.599 \pm 0.003) \times 10^{-7}. \quad (40)$$

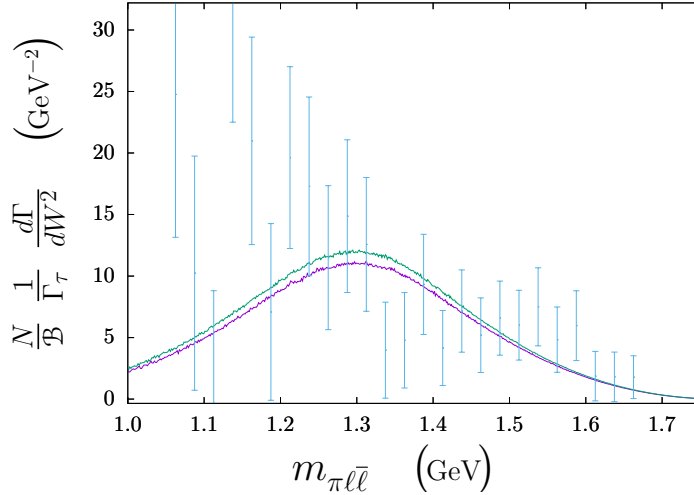


Figure 4: Normalized invariant mass spectra obtained with the two sets of parameters obtained from fitting to the Belle data. The purple line corresponds to the data with F_A fixed, while the green one stands for that with λ_0^* fixed. The blue data corresponds to measurements of τ^- decays, which show best agreement with our model. [7]

	set 1	set 2
	$F_A = 130 \text{ MeV}$	$\lambda_0^* = 102 \times 10^{-3}$
F_A	130 MeV	$(122 \pm 0) \text{ MeV}$
F_V	$(135.5 \pm 1.1) \text{ MeV}$	$(137.4 \pm 1.6) \text{ MeV}$
λ_0^*	$(384 \pm 0) \times 10^{-3}$	102×10^{-3}
\mathcal{B}	$(6.01 \pm 0) \times 10^{-6}$	$(6.36 \pm 0.12) \times 10^{-6}$
χ^2/dof	31.1/26	31.4/26

Table 1: Our best fit results for F_A , F_V , λ_0^* and the branching ratio. For the fit results shown on the left (right) columns we fix $F_A = 130 \text{ MeV}$ ($\lambda_0^* = 102 \times 10^{-3}$), respectively. A 0 error means that the fit uncertainty in the parameter is negligible with respect to its central value.

As expected, it is a factor ~ 37 smaller than the Belle measurement, which confirms $m_{\pi^-e^+e^-} \geq 1.05 \text{ GeV}$ is a good cut to study structure-dependent effects.

Thus, the \mathcal{B} adding the SI contribution gives the total branching ratios shown in table 2, where the first (dominant) error includes the uncertainty from unfolding and from the difference between \mathcal{B} and BR and the second error was obtained from the Gaussian distribution of the fitted parameters. Also, in the same table, we show the SI contributions to the branching fractions for the different decay channels in the complete phase space.

P, ℓ	$\mathcal{B}(\tau \rightarrow \nu_\tau P \ell \bar{\ell})$		IB
	set 1	set 2	
π, e	$(2.38 \pm 0.28 \pm 0.11) \cdot 10^{-5}$	$(2.45 \pm 0.45 \pm 0.04) \cdot 10^{-5}$	$1.457(5) \cdot 10^{-5}$
π, μ	$(8.45 \pm 2.45 \pm 1.09) \cdot 10^{-6}$	$(9.15 \pm 3.25 \pm 0.25) \cdot 10^{-6}$	$1.5935(4) \cdot 10^{-7}$
K, e	$(1.17 \pm 0.26 \pm 0.09) \cdot 10^{-6}$	$(1.11 \pm 0.28 \pm 0.04) \cdot 10^{-6}$	$3.225(5) \cdot 10^{-7}$
K, μ	$(6.4 \pm 1.9 \pm 0.8) \cdot 10^{-7}$	$(5.85 \pm 1.75 \pm 0.20) \cdot 10^{-7}$	$3.4191(8) \cdot 10^{-9}$

Table 2: Branching ratios for the different τ decay channels. In the middle columns, our prediction for the full branching ratio accounting for both (dominant) systematic and statistical uncertainties (see main text). In the right column we show the SI contribution with the error arising from numerical integration of the differential decay width.

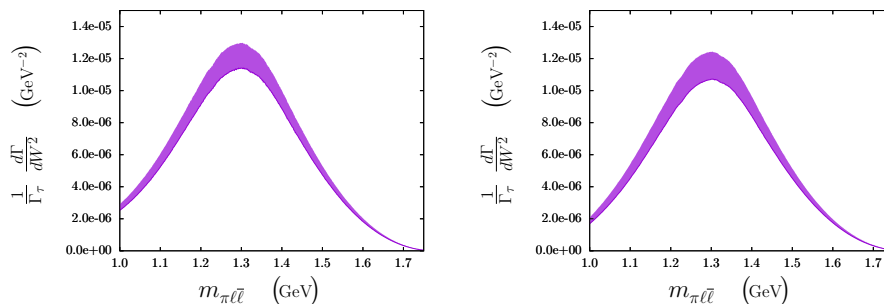


Figure 5: Invariant mass spectra $m_{\pi^-e^+e^-}$ for $P = \pi$, the thickness represents the error band obtained from the difference between the two sets. The plot in the left is for $\ell = e$, while the other is for $\ell = \mu$.

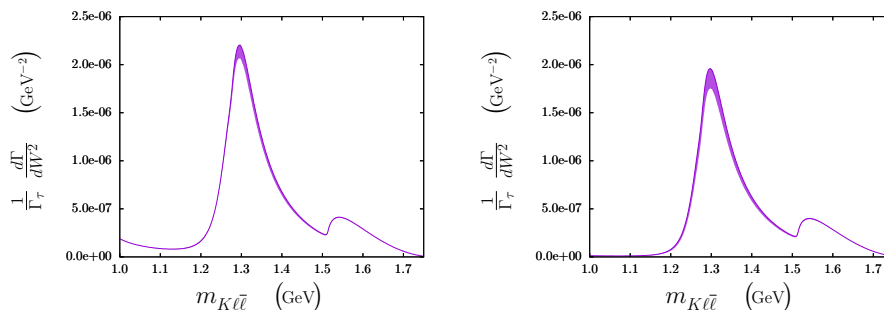


Figure 6: Same as Figure 5 for $P = K$.

From the discussion at the beginning of section 4.2 and from the results shown in table 2, we take the \mathcal{B} of each decay channel to be within the range obtained from the union of the intervals given by each set of fitted parameters,

the latter ranges defined as the intervals given by each central value of Table 2 and its uncertainties. Also, we computed the W^2 spectra for the different decay channels shown in Figures 5 and 6 using both sets of fitted parameters, where the error band was obtained by taking the difference between them. The same was done for the s_{34} spectra in Figures 7 and 8. Measurement of these observables at Belle-II [56] will be crucial for further reducing the uncertainties shown.

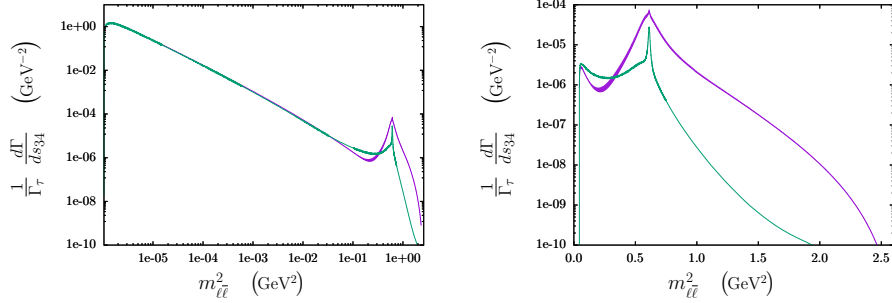


Figure 7: Invariant mass spectra $m_{\ell\bar{\ell}}$ for $P = \pi$, the thickness of the purple line represents the error band obtained from the difference between the two sets. The green line is the prediction of ref. [5]. The left-hand plot is for $\ell = e$, while the other is for $\ell = \mu$.

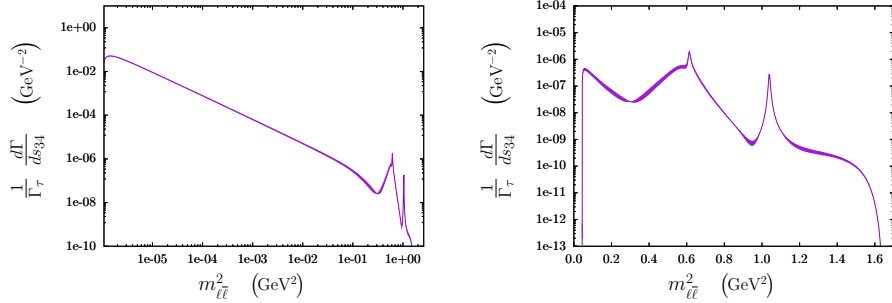


Figure 8: Invariant mass spectra $m_{\ell\bar{\ell}}$ for $P = K$, the thickness of the purple line represents the error band obtained from the difference between the two sets. The plot on the left is for $\ell = e$, while the other is for $\ell = \mu$.

5 Conclusions

Motivated by recent measurements of the Belle Collaboration [7], in this paper we present an improved prediction of the $\tau^- \rightarrow \pi^- e^+ e^- \nu_\tau$ decay. This includes a more accurate description of the structure-dependent parts of the decay am-

plitudes, by taking into account the first order flavor-breaking corrections to the form factors involved in the $W\pi\gamma^*$ vertex. As done for the VVP Green's function [30], we found that the inclusion of the pseudoscalar resonance is needed in order to obtain compatible expressions between the VAP Green's function and the form factors. In the high-energy limit we find that these expressions give the same constraints on the parameters of the resonance Lagrangians, as happens in the VVP case.

P, ℓ	$\mathcal{B}(\tau^- \rightarrow \nu_\tau P^- \ell \bar{\ell})$
π, e	$(2.41 \pm 0.40 \pm 0.12) \cdot 10^{-5}$
π, μ	$(9.15 \pm 3.25 \pm 1.12) \cdot 10^{-6}$
K, e	$(1.13 \pm 0.30 \pm 0.09) \cdot 10^{-6}$
K, μ	$(6.2 \pm 2.1 \pm 0.8) \cdot 10^{-7}$

Table 3: Branching ratios for the different decay channels. The central value is the mean of the union of intervals given in both columns of Table 2, the first error covers the width of such union of ranges (see discussion below eq. (40)) and the second error is the quadratic mean of statistical uncertainties in Table 2.

We have obtained a reasonably good fit of the parameters that remain unconstrained after applying the SD behaviour to the form factors. A better set of data for the invariant mass spectrum of the hadronic current would allow to determine physically meaningful parameters in a unique way. It is worth to recall that despite the fact that we had access to the $\tau^+ \rightarrow \bar{\nu}_\tau \pi^+ e^+ e^-$ spectra obtained from Belle, we found some inconsistencies that make unreliable the fits to data from both positive and negative tau decays (see discussion in section 4.2). We have therefore only considered the data set of the τ^- decays. From the results in Table 2, we conclude that our best result for the branching fractions is the union of ranges given for both fitting sets. This is shown in Table 3, where the central value is the mean of the union of these intervals. The results for the $P = \pi$ case agree with those in ref. [5], where $(1.7_{-0.3}^{+1.1}) \cdot 10^{-5}$ for $\ell = e$ and $[3 \cdot 10^{-7}, 1 \cdot 10^{-5}]$ for $\ell = \mu$ were predicted. Thus, we have reached a more precise determination of the branching ratios for the π decay channels than the previous ones in ref. [5]. Also, similar observables for the $\tau^\pm \rightarrow \nu_\tau K^\pm \ell \bar{\ell}$ channels are predicted for the first time.

Despite the great achievement of the Belle collaboration [7] discovering the $\tau^- \rightarrow \nu_\tau \pi^- e^+ e^-$ decays, our study shows the need for better data (hopefully from Belle-II [56] and forthcoming facilities) in order to increase our knowledge of these decay modes. The $m_{\pi^- e^+ e^-}$ spectrum shown in Figure 4 is consistent with the destructive interference of the $\rho(1450)$ and $\rho(1700)$ resonances; however, current data uncertainties prevent investigating the dynamics involved in the interplay of such resonances. The effect of ρ excitations does not seem, however, negligible, since by imposing the known behaviour [30] $F_V = \sqrt{3}F$ to

the fit gives a far worse χ^2 than those in Table 1, which are closer to $F_V = \sqrt{2}F$ (which holds with a minimal resonance Lagrangian beyond which we go in this and in our previous work on the subject). We assume that the effect of these heavier copies of the ρ meson are responsible for this shift in the value of F_V .

Acknowledgements

We are indebted to Denis Epifanov and Yifan Jin for leading the Belle analysis of these decays, and measuring for the first time the $\tau \rightarrow \pi e^+ e^- \nu_\tau$ decays. We specially acknowledge Yifan Jin for sharing with us detailed information on their study and providing us with the simulated Monte Carlo generation. A.G. was supported partly by the Spanish MINECO and European FEDER funds (grant FIS2017-85053-C2-1-P) and Junta de Andalucía (grant FQM-225) and partly by the Generalitat Valenciana (grant Prometeo/2017/053). G.L.C. acknowledges funding from Ciencia de Frontera Conacyt project No. 428218, and P.R. by the SEP-Cinvestav Fund (project number 142), and by Cátedras Marcos Moshinsky (Fundación Marcos Moshinsky), that also supported A. G.

References

- [1] A. Guevara, G. López-Castro and P. Roig, Phys. Rev. D **95** (2017) no.5, 054015.
- [2] T. Husek, K. Kampf, S. Leupold and J. Novotny, Phys. Rev. D **97** (2018) no.9, 096013.
- [3] K. Kampf, J. Novotný and P. Sánchez-Puertas, Phys. Rev. D **97** (2018) no.5, 056010.
- [4] A. Guevara, G. López Castro, P. Roig and S. L. Tostado, Phys. Rev. D **92** (2015) no.5, 054035.
- [5] P. Roig, A. Guevara and G. López Castro, Phys. Rev. D **88** (2013) no.3, 033007.
- [6] J. Bijnens, G. Ecker and J. Gasser, Nucl. Phys. B **396** (1993), 81-118.
- [7] Y. Jin *et al.* [Belle], Phys. Rev. D **100** (2019) no.7, 071101.
- [8] J. L. Gutiérrez Santiago, G. López Castro and P. Roig, Phys. Rev. D **103** (2021) no.1, 014027.
- [9] A. Flores-Tlalpa, G. Lopez Castro and P. Roig, J. High Energ. Phys. 2016, 185 (2016).
- [10] M. A. Arroyo-Ureña, G. Hernández-Tomé, G. López-Castro, P. Roig and I. Rosell, [arXiv:2107.04603 [hep-ph]], to be published in Phys. Rev. D, and work in progress.

- [11] T. Aoyama *et al.*, The Muon $g-2$ Theory Initiative, Phys. Rept. 887 (2020) 1-166.
- [12] G. Ecker, J. Gasser, A. Pich and E. de Rafael, Nucl. Phys. B **321** (1989), 311-342.
- [13] G. Ecker, J. Gasser, H. Leutwyler, A. Pich and E. de Rafael, Phys. Lett. B **223** (1989), 425-432.
- [14] J. Gasser and H. Leutwyler, Annals Phys. **158** (1984), 142.
- [15] J. Gasser and H. Leutwyler, Nucl. Phys. B **250** (1985), 465-516.
- [16] S. Weinberg, Physica A **96** (1979) no.1-2, 327-340.
- [17] A. Guevara, P. Roig and J. J. Sanz-Cillero, JHEP **06** (2018), 160.
- [18] P. Roig, A. Guevara and G. López Castro, Phys. Rev. D **89** (2014) no.7, 073016.
- [19] V. Cirigliano, G. Ecker, M. Eidemüller, R. Kaiser, A. Pich and J. Portolés, Nucl. Phys. B **753** (2006), 139-177.
- [20] M. Knecht and A. Nyffeler, Eur. Phys. J. C **21** (2001), 659-678.
- [21] V. Cirigliano, G. Ecker, M. Eidemüller, A. Pich and J. Portolés, Phys. Lett. B **596** (2004), 96-106.
- [22] V. Bernard, N. Kaiser and U. G. Meissner, Nucl. Phys. B **364** (1991), 283-320.
- [23] J. J. Sanz-Cillero, Phys. Rev. D **70** (2004), 094033.
- [24] Z. H. Guo and J. J. Sanz-Cillero, Phys. Rev. D **89** (2014) no.9, 094024.
- [25] J. Wess and B. Zumino, Phys. Lett. B **37** (1971), 95-97.
- [26] E. Witten, Nucl. Phys. B **223** (1983), 422-432.
- [27] J. Bijnens, L. Girlanda and P. Talavera, Eur. Phys. J. C **23** (2002), 539-544.
- [28] K. Kampf and J. Novotny, Phys. Rev. D **84** (2011), 014036.
- [29] J. Bijnens, G. Colangelo and G. Ecker, JHEP **02** (1999), 020.
- [30] P. Roig and J. J. Sanz Cillero, Phys. Lett. B **733** (2014), 158-163.
- [31] T. Kadavý, K. Kampf and J. Novotny, JHEP **10** (2020), 142.
- [32] P. D. Ruiz-Femenía, A. Pich and J. Portolés, JHEP **07** (2003), 003.
- [33] D. Gómez Dumm, A. Pich and J. Portolés, Phys. Rev. D **69** (2004), 073002.
- [34] V. Cirigliano, G. Ecker, H. Neufeld and A. Pich, JHEP **06** (2003), 012.

- [35] Z. H. Guo and J. J. Sanz-Cillero, Phys. Rev. D **79** (2009), 096006.
- [36] D. Gómez Dumm, A. Pich and J. Portolés, Phys. Rev. D **62** (2000), 054014.
- [37] M. Jamin, A. Pich and J. Portolés, Phys. Lett. B **640** (2006), 176-181.
- [38] D. G. Dumm, P. Roig, A. Pich and J. Portolés, Phys. Lett. B **685** (2010), 158-164.
- [39] I. M. Nugent, T. Przedzinski, P. Roig, O. Shekhovtsova and Z. Was, Phys. Rev. D **88** (2013), 093012.
- [40] D. G. Dumm, P. Roig, A. Pich and J. Portolés, Phys. Rev. D **81** (2010), 034031.
- [41] P. A. Zyla *et al.* [Particle Data Group], PTEP **2020** (2020) no.8, 083C01.
- [42] Z. H. Guo, Phys. Rev. D **78** (2008), 033004.
- [43] D. Gómez Dumm and P. Roig, Phys. Rev. D **86** (2012), 076009.
- [44] Z. H. Guo and P. Roig, Phys. Rev. D **82** (2010), 113016.
- [45] G. P. Lepage and S. J. Brodsky, Phys. Rev. D **22** (1980), 2157.
- [46] S. J. Brodsky and G. R. Farrar, Phys. Rev. Lett. **31** (1973), 1153-1156.
- [47] V. Cirigliano and I. Rosell, JHEP **10** (2007), 005.
- [48] B. Moussallam, Nucl. Phys. B **504** (1997), 381-414.
- [49] M. Jamin, J. A. Oller and A. Pich, Nucl. Phys. B **587** (2000), 331-362.
- [50] M. Jamin, J. A. Oller and A. Pich, Nucl. Phys. B **622** (2002), 279-308.
- [51] M. F. L. Golterman and S. Peris, Phys. Rev. D **61** (2000), 034018.
- [52] O. Shekhovtsova, T. Przedzinski, P. Roig and Z. Was, Phys. Rev. D **86** (2012), 113008.
- [53] S. Antropov, S. Banerjee, Z. Was and J. Zaremba, [arXiv:1912.11376 [hep-ph]].
- [54] J. A. Miranda and P. Roig, Phys. Rev. D **102** (2020), 114017.
- [55] V. Mateu and J. Portolés, Eur. Phys. J. C **52** (2007), 325-338.
- [56] E. Kou *et al.* [Belle-II], PTEP **2019** (2019) no.12, 123C01; PTEP **2020** (2020) 2, 029201 (erratum).